Josephson junction with noise

V. Berdichevsky and M. Gitterman
Department of Physics, Bar-Ilan University, Ramat Gan 52900, Israel
(Received 30 May 1997)

We analyze the voltage-current characteristics of a Josephson junction subject to multiplicative noise with and without additive noise. An analytical solution was obtained for the dichotomous multiplicative noise as well as for the forms of the voltage-current characteristics for different noise amplitudes and rates. Nonmonotonic behavior was found for the voltage as a function of noise rate (stochastic resonance). The cooperative action of additive and multiplicative noises results in a voltage larger than that predicted from Ohm's law. The ratchet effect and limit cases of weak and strong noises are analyzed in detail. [S1063-651X(97)06011-X]

PACS number(s): 05.40.+j

I. INTRODUCTION

The resistively shunted Josephson junction is usually assumed small so that the current is uniform over its cross section. The application of Kirchoff's law to such a circuit gives the following equation:

$$J=J_c \sin\varphi+\frac{V(t)}{R}=J_c \sin\varphi+\frac{\hbar}{2eR}\frac{d\varphi}{dt}, \tag{1}$$

where the Josephson relation $\varphi(t)=(2e/\hbar)\int V dt$ has been used. We obtained Eq. (1) in the diffusion (or noninertial, or low-frequency) limit in which one can neglect the capacitance C of the Josephson circuit. Otherwise, the term $C(dV/dt)\equiv(C\hbar/2e)d^2\varphi/dt^2$ appears on the right-hand side of Eq. (1). We neglect this term in our calculation, thereby considering the so-called overdamped case.

One can rewrite Eq. (1) in dimensionless form as

$$\frac{d\varphi}{dt}=J-J_c \sin\varphi, \tag{2}$$

where the dc current J and the critical current J_c are measured in units of $\hbar/2eR$, where R is the resistivity of the junction. Comparison with the microscopic theory gives [1]

$$J_c=\frac{e\hbar\Delta}{\lambda}\tanh\left(\frac{\Delta}{T}\right), \tag{3}$$

where Δ is the absolute value of the order parameter, and λ is the correlation length.

The solution of Eq. (2) is easily found. The most important property of this solution is the voltage-current characteristic of a Josephson junction. The voltage across a junction is proportional to $d\varphi/dt\equiv\dot{\varphi}$, and we readily find from Eq. (2) that

$$\langle\dot{\varphi}\rangle\equiv\lim_{T\to\infty}\frac{1}{T}\int_0^T\varphi(\tau)d\tau=\begin{cases}0, & J<J_c\\ \sqrt{J^2-J_c^2}, & J>J_c.\end{cases} \tag{4}$$

Equation (4), shown by the solid line in Fig. 1, can be easily understood in terms of an overdamped driven pendulum, which is also described by Eq. (2). When the external torque J is small, the pendulum can only perform small oscillations around its equilibrium point, while for large J, the pendulum is able to execute complete rotations.

Notice that the generic equation (2) appears in a number of different applications, such as the theory of charge density waves [2], phase locking in electric circuits [3], mode locking in ring laser gyroscopres [4], motion of fluxons in superconductors [5], and the penetration of biological channels by ions [6]. Therefore, our analysis is also applicable to all these problems.

If an additional periodic force (due to the ac current or radiation) is acting on a junction, apart from the dc current J, then new interesting phenomena occur. One of the most remarkable is the lock-in phenomenon of oscillators, which manifests itself as horizontal ''Shapiro steps'' in the voltage-current characteristic of Josephson junctions. In fact, Eq. (4) defines the zero Shapiro step. One can calculate the sizes of these steps for a single sinusoid, $\sin(\omega t)$, by perturbation theory or by numerical solution, while their positions are given by $\langle\dot{\varphi}\rangle=n\omega$, $n=1,2,3,\ldots$. If the external force has the form of a pulse signal, one can calculate exactly the sizes of Shapiro steps [5].

So far we have considered only deterministic quantities. However, all physical parameters are subject to random perturbations. Two typical parameters of superconductors that enter Eqs. (2) and (3), the phase φ, and the absolute value Δ of the order parameter, are also susceptible to fluctuations. This fact can be taken into account by including random forces in Eq. (2):

$$\frac{d\varphi}{dt}=[J+f_1(t)]-[J_c+f_2(t)]\sin(\varphi). \tag{5}$$

The additive noise $f_1(t)$, for example, comes from the thermal fluctuations. The influence of these fluctuations on the voltage-current characteristics (4) has been considered under the assumption of the white [1,6] and the dichotomous [7,8] forms of noise $f_1(t)$ with $f_2(t)\equiv 0$.

In this paper we consider an additional generalization of Eq. (2), along with $f_1(t)$, allowing for fluctuations $f_2(t)$ of the critical current J_c. The latter are of special importance for high-temperature superconductors (HTSC). Many properties of HTSC can be described in terms of the dynamics of flux vortices [9]. Flux pinning in superconducting films is responsible for the high critical currents in these films. The

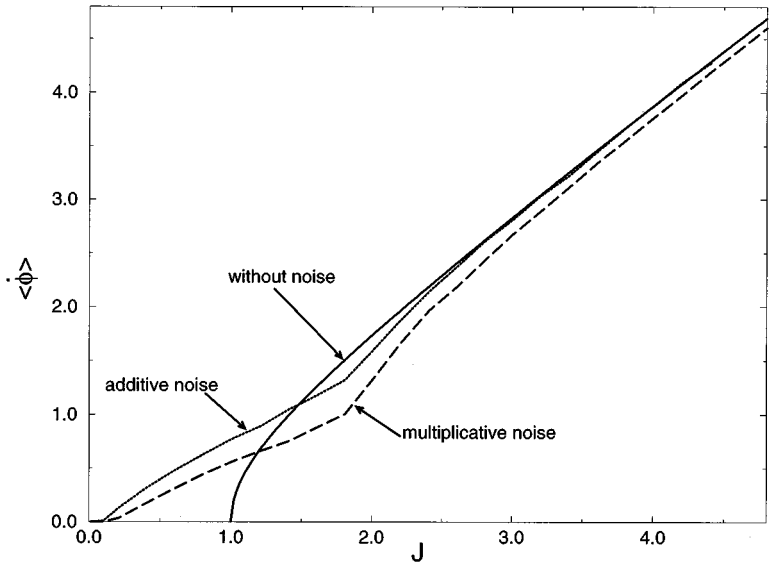

FIG. 1. Voltage-current characteristic of a Josephson junction without noise (solid line), with additive (dotted line), or with multiplicative (dashed line) dichotomous noises. The parameters have the following values: $J_c=1$, $A_1=B_1=A_2=B_2=0.9$; $\alpha=\beta=0.1$.

different pinning centers, which, in turn, give rise to different J_c, are produced by structural disorders in HTSC, such as twinning planes, random distribution of oxygen vacancies, etc. Experimental manifestations of these phenomena are low-frequency noise measurements of the fluxon motion [10] and of the voltage noise induced by vortex motion [11]. Results of both types of measurements suggest the existence of $1/f$ noise and random telegraph signals. Such signals have been observed in granular YBa_2Cu_3O (YBCO) films at liquid-helium temperature [12] and in $BiSr_xCa_{1-x}CuO$ (BSCCO) films at temperatures just below the critical temperature [13]. It is now generally accepted that random telegraph signals can arise from the thermally activated hopping of a single magnetic vortex between two distinct pinning sites [14].

Another explanation for the fluctuating critical current is the intrinsic Josephson mechanism. The HTSC thin film can be modeled as a two-dimensional network of superconducting grains linked by Josephson coupling. A change in the flux is able to change the critical current of a Josephson junction. Fluctuations between two distinct sites correspond to fluctuations of the critical current between two values J_{c_1} and J_{c_2}. Indirect support for the Josephson mechanism is lent by the observation [15] that random telegraph signals have been observed only when the biased current exeeds a critical threshold, as follows from Eq. (4).

In this paper we investigate the effect of different types of noise on the current-voltage characteristics (4) of a Josephson junction.

The random quantities $f_1(t)$ and $f_2(t)$ have zero mean values,

$$\langle f_1(t)\rangle=\langle f_2(t)\rangle=0. \tag{6}$$

Their correlation properties can be either ''white'' or ''colored.'' For white noise,

$$\langle f(t)f(t')\rangle=2D\,\delta(t-t'), \tag{7}$$

while for the colored noise, we shall restrict our consideration to the case of exponentially correlated noise

$$\langle f(t)f(t')\rangle\sim\exp[-2\gamma|t-t'|]. \tag{8}$$

As the simplest example of colored noise, we consider dichotomous noise (random telegraph signal) for which the random variable $f(t)$ can have either of two values, A or $-B$. The rate for the (random) transitions $A\rightarrow -B$ will be denoted by γ_1, and the reverse rate will be denoted by γ_2.

The latter condition means that we assume an exponential function for the switch probability between two states

$$\Psi_i=\gamma_i e^{-\gamma_i t},\quad i=1,2, \tag{9}$$

where γ_i^{-1} is the average time between switches.

The correlation function of the dichotomous noise then has the following form:

$$\langle f(t)f(t')\rangle=AB\,\exp[-(\gamma_1+\gamma_2)|t-t'|]. \tag{10}$$

In order to satisfy the condition of zero mean value (6), the following relation between the parameters is implied:

$$\gamma_2 A=\gamma_1 B. \tag{11}$$

The white-noise limit (7) of the dichotomous noise (9) can be obtained from the following limits

$$A=|B|\equiv\Delta\rightarrow\infty,\quad \gamma_1=\gamma_2\equiv\gamma\rightarrow\infty,\quad \lim\frac{\Delta^2}{2\gamma}=D. \tag{12}$$

This paper is organized as follows. In Sec. II, we derive the general Fokker-Planck equations, which correspond to the Langevin equations (5) when both noises, $f_1(t)$ and $f_2(t)$, are dichotomous, leaving for the Appendix the derivation of the Fokker-Planck equations for the more general case (8) of the exponentially correlated noises.

In Secs. III and IV, we analyze separately additive and multiplicative noise. Some important differences between these two cases will be emphasized. The voltage-current characteristics under the concurrent influence of both types of noise is studied in Sec. V. Section VI contains different forms of solutions of the Fokker-Planck equation convenient for the analysis of the limiting cases of weak and strong noises. Finally, Sec. VII contains our conclusions.

II. GENERAL EQUATIONS

In order to consider the effects of additive and multiplicative dichotomous noise on the dynamics of a Josephson junction, we first derive the Fokker-Planck equations corresponding to the Langevin equation (5). To this end, we assume that both $f_1(t)$ and $f_2(t)$ are dichotomous noise, with zero mean value (6) and correlators (10) of the form

$$\langle f_1(t)f_1(t')\rangle = A_1B_1 \exp[-(\alpha_1+\alpha_2)|t-t'|],$$
$$\langle f_2(t)f_2(t')\rangle = A_2B_2 \exp[-(\beta_1+\beta_2)|t-t'|]. \quad (13)$$

According to Eq. (11),

$$\alpha_2A_1=\alpha_1B_1, \quad \beta_2A_2=\beta_1B_2. \quad (14)$$

Equation (5) describes, in fact, four different functions $\varphi_i(t)$ with equations resulting when $f_1(t), f_2(t)$ take all pair combinations of $A_1, -B_1$ and $A_2, -B_2$, respectively. These functions are random, due to random switches between different states. Therefore, their properties can be described by four probabilities, $P_1(\varphi,t|A_1,A_2)$, $P_2(\varphi,t|A_1,B_2)$, $P_3(\varphi,t|B_1,A_2)$, and $P_4(\varphi,t|B_1,B_2)$, where the probability that $\varphi<\varphi(t)\leqslant\varphi+d\varphi$ is equal to $P_i(\varphi,t)d\varphi$. In general, such a probability must be calculated as the solution of an integral equation. However, choosing the switch probability to have a form shown in Eq. (9) simplifies our analysis to the Markovian form and reduces the integral equations to differential equations. The four equations for $P_i(\varphi,t)$ are derived by enumerating the ways in which these functions change with time. For the case of two states, the appropriate procedure was considered in detail in Ref. [7]. We obtain the coupled equations for the $P_i(\varphi,t)$, involving the dynamic part defined by Eq. (5) and the transition rates shown in Eq. (9),

$$\frac{\partial P_1}{\partial t} = -\frac{\partial}{\partial\varphi}\{[g(\varphi)-A_2\sin(\varphi)+A_1]P_1\}+\beta_2P_2-\beta_1P_1 + \alpha_2P_3-\alpha_1P_1,$$
$$\frac{\partial P_2}{\partial t} = -\frac{\partial}{\partial\varphi}\{[g(\varphi)+B_2\sin(\varphi)+A_1]P_2\}+\beta_1P_1-\beta_2P_2 + \alpha_2P_4-\alpha_1P_2,$$
$$\frac{\partial P_3}{\partial t} = -\frac{\partial}{\partial\varphi}\{[g(\varphi)-A_2\sin(\varphi)-B_1]P_3\}+\alpha_1P_1-\alpha_2P_3 + \beta_2P_4-\beta_1P_3,$$
$$\frac{\partial P_4}{\partial t} = -\frac{\partial}{\partial\varphi}\{[g(\varphi)+B_2\sin(\varphi)-B_1]P_4\}+\alpha_1P_2-\alpha_2P_4 + \beta_1P_3-\beta_2P_4, \quad (15)$$

where

$$g(\varphi)=J-J_c\sin(\varphi). \quad (16)$$

It is useful to replace this set of equations by an equivalent set of equations for the functions

$$P=P_1+P_2+P_3+P_4,$$
$$X=A_1(P_1+P_2)-B_1(P_3+P_4),$$
$$Y=B_2(P_2+P_4)-A_2(P_1+P_3),$$
$$Z=A_1B_2P_2+A_2B_1P_3-B_1B_2P_4-A_1A_2P_1. \quad (17)$$

These functions are found from Eq. (15) to satisfy the following equations:

$$\frac{\partial P}{\partial t} = -\frac{\partial}{\partial\varphi}[g(\varphi)P+X-Y\sin(\varphi)]\equiv-\frac{\partial W}{\partial\varphi},$$
$$\frac{\partial X}{\partial t} = -\alpha X-\frac{\partial}{\partial\varphi}[g(\varphi)X+(A_1-B_1)X+A_1B_1P+Z\sin(\varphi)]$$
$$\frac{\partial Y}{\partial t} = -\beta Y-\frac{\partial}{\partial\varphi}[g(\varphi)Y-(A_2-B_2)Y\sin(\varphi) + A_2B_2P\sin(\varphi)+Z],$$
$$\frac{\partial Z}{\partial t} = -(\alpha+\beta)Z-\frac{\partial}{\partial\varphi}[g(\varphi)Z+(A_1-B_1)Z+A_1B_1Y - (A_2-B_2)Z\sin(\varphi)+A_2B_2X\sin(\varphi)], \quad (18)$$

where $\alpha=\alpha_1+\alpha_2$ and $\beta=\beta_1+\beta_2$.

The variable W in the first of these equations is seen to be a flux, since the function P is the full probability density. For the stationary state, the flux W is a constant that, as it will now be shown, defines the voltage-current characteristic of the Josephson junction. Let the stationary solution of (15) be denoted by $P_i^{\rm st}(\varphi)$, $i=1,2,3,4$. Then, the average of the periodic function $\dot\varphi$ can be written as follows:

$$\langle\dot\varphi\rangle = \int_{-\pi}^{\pi}\{[g(\varphi)-A_2\sin(\varphi)+A_1]P_1^{\rm st} + [g(\varphi)+B_2\sin(\varphi)+A_1]P_2^{\rm st} + [g(\varphi)-A_2\sin(\varphi)-B_1]P_3^{\rm st} + [g(\varphi)+B_2\sin(\varphi)-B_1]P_4^{\rm st}\}d\varphi = \int_{-\pi}^{\pi}[g(\varphi)P^{\rm st}-Y^{\rm st}\sin(\varphi)+X^{\rm st}]d\varphi = 2\pi W. \quad (19)$$

Therefore, our main goal will be to solve Eqs. (18) for the stationary case (setting the time derivatives equal to zero) under the appropriate conditions of periodicity and normalization. However, before proceeding further let us rewrite Eqs. (18) for some special cases.

Symmetric dichotomous noise

If the dichotomous noises are symmetric, i.e., $A_1=|B_1|$ and $A_2=|B_2|$ [i.e., according to Eq. (14), $\alpha_1=\alpha_2\equiv\alpha$ and $\beta_1=\beta_2\equiv\beta$], then for the stationary case, Eqs. (18) reduce to the following form (for simplicity we omit the superscript ''st'' for the functions P, X, Y, and Z):

$$W=g(\varphi)P+X+Y\ \sin(\varphi), \tag{20}$$

$$-\alpha X-\frac{\partial}{\partial\varphi}[g(\varphi)X+A_1^2P+Z\ \sin(\varphi)]=0, \tag{21}$$

$$-\beta Y-\frac{\partial}{\partial\varphi}[g(\varphi)Y+A_2^2\ \sin(\varphi)P+Z]=0, \tag{22}$$

$$-(\alpha+\beta)Z-\frac{\partial}{\partial\varphi}[g(\varphi)Z+A_1^2Y+A_2^2X\ \sin(\varphi)]=0. \tag{23}$$

White noise

Additional simplification can be achieved by going from dichotomous to white noise using Eq. (12). Denoting $D_1=\lim_{\alpha,A_1\to\infty}A_1^2/2\alpha$ and $D_2=\lim_{\beta,A_2\to\infty}A_2^2/2\beta$, one obtains from Eqs. (21) and (22), $X=-D_1\,dP/d\varphi$ and $Y=-D_2\,(d/d\varphi)[P\ \sin(\varphi)]$. Substituting the latter formulas into Eq. (20) and rearranging terms, one finds

$$\frac{dP}{d\varphi}+\Gamma(\varphi)P=W\Omega(\varphi), \tag{24}$$

where

$$\Gamma(\varphi)=-\frac{g(\varphi)-(D_2/2)\sin(2\varphi)}{D_1+D_2\ \sin^2(\varphi)},$$

$$\Omega(\varphi)=-[D_1+D_2\ \sin^2(\varphi)]^{-1}. \tag{25}$$

Equation (24) is a generic equation to which we will refer later on. Using this equation as an example, we illustrate the further calculations.

The solution of the first-order differential equation (24) contains one arbitary constant. This constant, as well as W, can be found from the normalization and periodicity conditions

$$\int_{-\pi}^{\pi}P(\varphi)d\varphi=1\quad\text{and}\quad P(-\pi)=P(\pi). \tag{26}$$

Finally, one gets for the voltage $\langle\dot\varphi\rangle=2\pi W$

$$\langle\dot\varphi\rangle=2\pi\left[\int_0^{2\pi}\frac{e^{-\int_0^{\varphi}\Gamma(z)dz}}{e^{\int_{\varphi}^{\varphi+2\pi}\Gamma(z)dz}-1}\left(\int_{\varphi}^{\varphi+2\pi}\Omega(u)e^{\int_0^{u}\Gamma(z)dz}du\right)d\varphi\right]^{-1}. \tag{27}$$

We will return later to the analysis of these formulas.

III. ADDITIVE DICHOTOMOUS NOISE

Although the following case was already considered in the literature, we present it here as an example of our approach, and consider the limiting cases of weak and strong noise. Let us first consider white noise.

White noise

For the limiting case of white noise, Eq. (27) reduces to [6,7]

$$\langle\dot\varphi\rangle=2\pi D_1(1-e^{2\pi J/D_1})\left\{\int_{-\pi}^{\pi}\exp\left[\frac{1}{D_1}\int_{-\pi}^{\xi}g(\rho)d\rho\right]\left[\int_{\xi}^{\xi+2\pi}\exp\left(-\frac{1}{D_1}\int_{-\pi}^{z}g(\rho)d\rho\right)dz\right]d\xi\right\}^{-1}. \tag{28}$$

Additive dichotomous noise

In the general case of additive dichotomous noise in the absence of multiplicative noise ($A_2=B_2=\beta=0$), one can reduce Eq. (18) in the stationary case to the following form:

$$W=g(\varphi)P+X,$$

$$0=\alpha X+\frac{\partial}{\partial\varphi}[g(\varphi)X+(A_1-B_1)X+A_1B_1P]. \tag{29}$$

A simple calculation shows that Eq. (29) can be further reduced to Eq. (24) with

$$\Gamma(\varphi)=\frac{g'[2g+(A_1-B_1)]+\alpha g}{g[g+(A_1-B_1)]-A_1B_1}\quad\text{and}\quad\Omega(\varphi)=\frac{g'+\alpha}{g[g+(A_1-B_1)]-A_1B_1}, \tag{30}$$

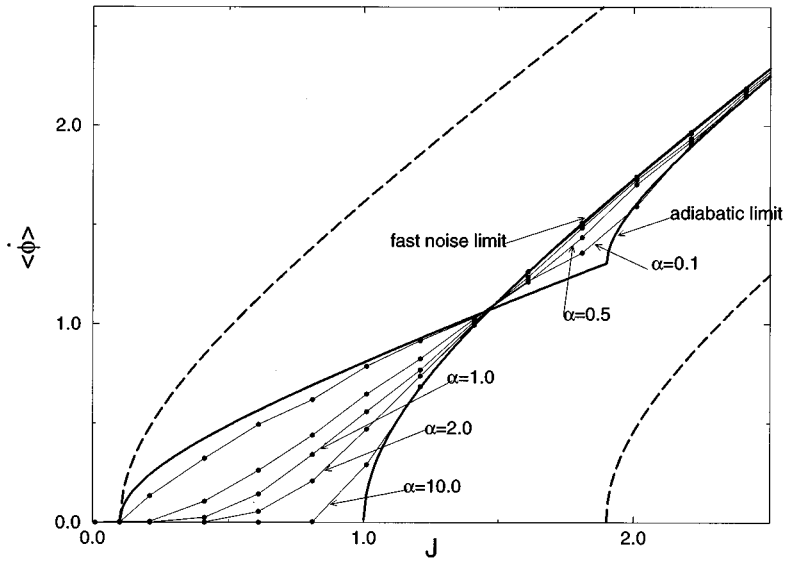

FIG. 2. Voltage-current characteristic of a Josephson junction subject to additive dichotomous noise for different values of the noise rate α between the adiabatic ($\alpha\to 0$) and the fast-noise ($\alpha\to\infty$) limits. The dashed curves refer to each of the two states. Parameters are $J_c=1$ and $A_1=B_1=0.9$.

i.e., the voltage-current characteristics $\langle\dot{\varphi}\rangle$ as a function of J will be given again by Eq. (27) with $\Gamma(\varphi)$ and $\Omega(\varphi)$ defined by Eq. (30).

Although the general voltage-current characteristic is quite cumbersome, its limit for slow jumps, $\alpha_1,\ \alpha_2\to 0$ (''adiabatic approximation''), has the following simple form:

$$\langle\dot{\varphi}\rangle\sim\begin{cases}0, & J-B_1 \quad\text{and}\quad J-A_1<J_c\\ \left(\dfrac{\sqrt{(J-B_1)^2-J_c^2}}{\alpha_2}+\dfrac{\sqrt{(J+A_1)^2-J_c^2}}{\alpha_1}\right)\Big/\left(\dfrac{1}{\alpha_1}+\dfrac{1}{\alpha_2}\right), & J-B_1 \quad\text{and}\quad J+A_1>J_c\\ \left(\dfrac{\sqrt{(J+A_1)^2-J_c^2}}{\alpha_1}\right)\Big/\left(\dfrac{1}{\alpha_1}+\dfrac{1}{\alpha_2}\right), & J-B_1<J_c \quad\text{and}\quad J+A_1>J_c.\end{cases}\tag{31}$$

These equations simply imply that in the adiabatic approximation, the total mobility is just an average of those for the two corresponding potentials [17–19].

The typical current-voltage characteristics of a Josephson junction subject to additive dichotomous noise are shown by the dotted line in Fig. 1, and—for different values of parameters—in Figs. 2 and 3. As one would expect, the presence of noise smeared out the sharp threshold behavior defined in Eq. (4), and this smearing depends on both the noise amplitude and the rate.

In Fig. 4, we show the voltage $\langle\dot{\varphi}\rangle$ as a function of noise rate α. This nonmonotonic behavior is a special manifestation of stochastic resonance [20], which was found for a bistable potential by Doering and Gadoua [22]. Note that in our case, this phenomenon occurs in a very narrow region of the bias current J.

Several conclusions can be drawn from this analysis.

(1) The voltage $\langle\dot{\varphi}\rangle$ does not vanish even for zero bias current, $J=0$. This phenomenon is a special case of the more general ''rachet effect'' for which the net transport (voltage in our case) is induced by nonequilibrium fluctuations when some asymmetry is present. These general conditions are obeyed in our case of nonsymmetric dichotomous noise. One can easily check that the rachet effect disappears in the limiting case of symmetric noise when $J=0$, which results in the vanishing of $\langle\dot{\varphi}\rangle$. The latter case occurs both for white noise, as follows immediately from Eq. (28), and for symmetric dichotomous noise, since the function $\Gamma(\varphi)$ defined in Eq. (30) is an odd function for $J=0$, and, according to Eq. (27), $\langle\dot{\varphi}\rangle=0$. The rachet effect might have practical application in superconducting electronics as well as in other fields of physics, chemistry, and biology (some recent references can be found in [8]).

(2) A stochastic resonance phenomenon (nonmonotonic behavior of the voltage as a function of noise rate) has been found in the narrow region of the bias current as shown in Fig. 4.

(3) For very large bias current, $J\gg J_c$, the voltage-current characteristics reduce to Ohm's law. Indeed, $g(\varphi)\approx J$, and this conclusion follows immediately from Eq. (2), i.e., $\langle\dot{\varphi}\rangle=J$.

(4) As will be shown in Sec. VI for white noise, the low-noise corrections to the voltage-current characteristic are different for $J>J_c$ and for $J<J_c$. In the former case, these

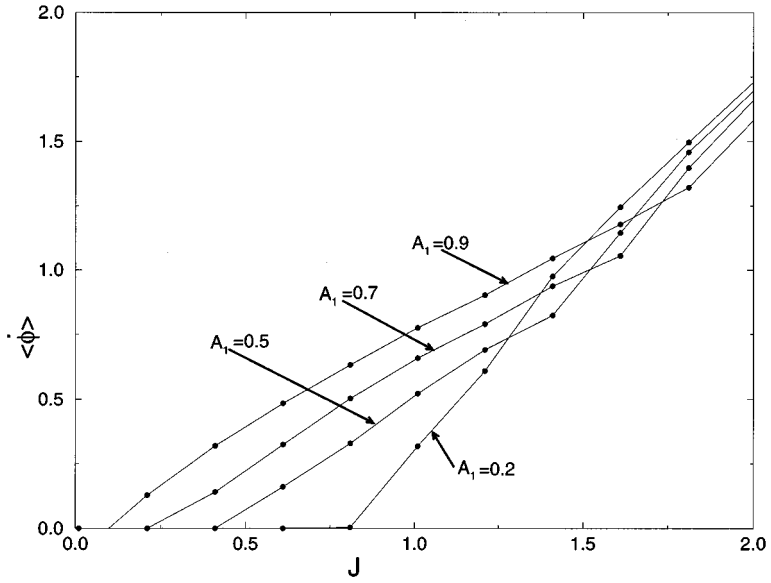

FIG. 3. Same as Fig. 2, but for different values of noise amplitudes A_1. Parameters are $J_c=1$ and $\alpha=0.1$.

corrections have an Arrenius-type form, whereas in the latter case, the form of polynomials. As one can easily see from Eqs. (24) and (30), this property also occurs in the general case of additive dichotomous noise.

IV. MULTIPLICATIVE DICHOTOMOUS NOISE

In the absence of additive noise, one has to put $A_1=B_1=\alpha=0$ in Eqs. (18), which for a stationary state will take the following form:

$$W=g(\varphi)P-Y\ \sin(\varphi),$$

$$-\beta Y-\frac{d}{d\varphi}[g(\varphi)Y-(A_2-B_2)Y\ \sin(\varphi)+A_2B_2\ \sin(\varphi)P]=0. \tag{32}$$

Solving Eqs. (32) for the stationary distribution function $P_{\mathrm{st}}(\varphi)$ of a Josephson junction subject to multiplicative noise where the critical current is allowed to take one of two values, $J_{c1}=J_c+A_2$ or $J_{c2}=J_c-B_2$, one obtains

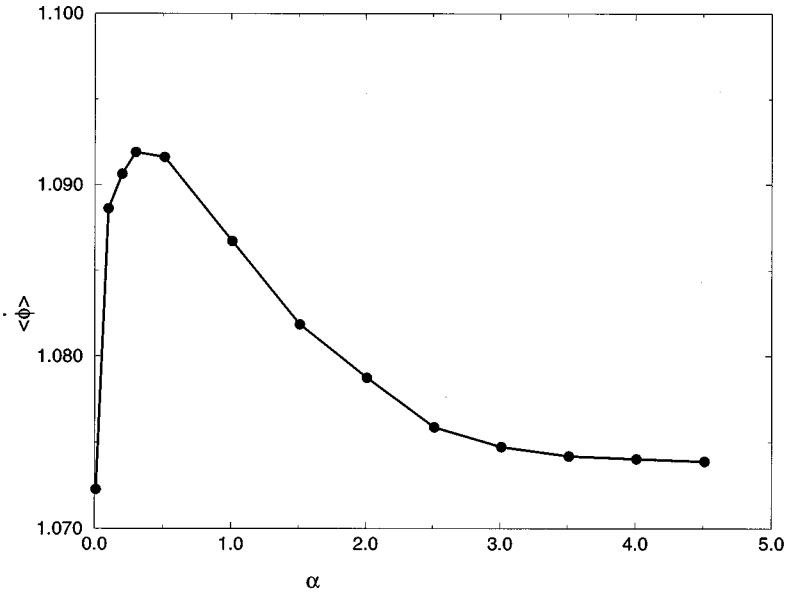

FIG. 4. Voltage $\langle\dot{\varphi}\rangle$ as a function of noise rate α for additive dichotomous noise. Parameters are $A_1=B_1=0.9$ and $J_c=1$.

$$P_{\rm st}(\varphi)=W\left[\frac{1}{J-[(J_{c1}+J_{c2})/2]\sin(\varphi)}+\frac{\Delta\ \sin(\varphi)U^{-1}(\varphi)I(\varphi)}{[J-J_{c1}\ \sin(\varphi)][J-J_{c2}\ \sin(\varphi)]}\right]-\frac{C\Delta\ \sin(\varphi)U^{-1}(\varphi)}{\beta[J-J_{c1}\ \sin(\varphi)][J-J_{c2}\sin(\varphi)]},\quad(33)$$

where

$$U(\varphi)=\exp\left[2\beta\int_u^{\varphi}\frac{J-[(J_{c1}+J_{c2})/2]\sin\varsigma}{[J-J_{c1}\ \sin(\varsigma)][J-J_{c2}\ \sin(\varsigma)]}d\varsigma\right],$$

$$I(\varphi)=\int_u^{\varphi}U(\varsigma)\frac{d}{d\varsigma}\left[\frac{(J_{c1}-J_{c2})\sin(\varsigma)}{2\{J-[(J_{c1}+J_{c2})/2]\sin(\varsigma)\}}\right]d\varsigma.\quad(34)$$

The probability function (33) is normalizable when

$$J>J_{c1},J_{c2}.\quad(35)$$

In this section we assume that the condition (35) is satisfied.

Using the normalization and periodicity conditions (26) in order to find constants C and W in Eq. (33), one obtains the following voltage-current characteristic:

$$\langle\dot\varphi\rangle=\left\{\frac{1}{2}\frac{1}{\sqrt{J^2-J_{c1}^2}}+\frac{1}{2}\frac{1}{\sqrt{J^2-J_{c2}^2}}-\frac{1}{4\pi}\int_u^{u+2\pi}\Psi_-(\varphi)\left[\alpha+\beta\int_u^{\varphi}\frac{(J_{c1}-J_{c2})\sin(\varsigma)}{2\{J-[(J_{c1}+J_{c2})/2]\sin(\varsigma)\}}\Psi_+(\varsigma)d\varsigma\right]d\varphi\right\}^{-1},\quad(36)$$

where

$$\Psi_{\pm}(\varphi)=\left[\frac{1}{J-J_{c1}\ \sin(\varphi)}\pm\frac{1}{J-J_{c2}\ \sin(\varphi)}\right]\exp\left[\pm\beta\int_u^{\varphi}\left(\frac{1}{J-J_{c1}\sin(\varsigma)}+\frac{1}{J-J_{c2}\ \sin(\varsigma)}\right)d\varsigma\right],$$

$$\alpha=\left[\beta\int_u^{u+2\pi}\Psi_+(\varsigma)\frac{(J_{c1}-J_{c2})\sin(\varsigma)}{2\{J-[(J_{c1}+J_{c2})/2]\sin(\varsigma)\}}d\varsigma\right]\left\{\exp\left[\beta\left(\frac{2\pi}{\sqrt{J^2-J_{c1}^2}}+\frac{2\pi}{\sqrt{J^2-J_{c2}^2}}\right)\right]-1\right\}^{-1}.\quad(37)$$

For $J_{c1}=J_{c2}$, Eq. (36) reduces to Eq. (4), as it should.

Analogous to Eq. (31), Eq. (36) can be also simplified in the limiting case of slow jumps between the potentials, $\beta\to0$ (adiabatic approximation):

$$\langle\dot\varphi\rangle\sim\begin{cases}\left(\dfrac{\sqrt{J^2-(J_c+A_2)^2}}{\beta_1}+\dfrac{\sqrt{J^2-(J_c-B_2)^2}}{\beta_2}\right)\Big/\left(\dfrac{1}{\beta_1}+\dfrac{1}{\beta_2}\right), & J>J_c+A_2\quad\text{and}\quad J>J_c-B_2\\ \left(\dfrac{\sqrt{J^2-(J_c-B_2)^2}}{\beta_2}\right)\Big/\left(\dfrac{1}{\beta_1}+\dfrac{1}{\beta_2}\right), & J<J_c+A_2\quad\text{and}\quad J>J_c-B_2\\ 0, & J<J_c+A_2\quad\text{and}\quad J<J_c-B_2.\end{cases}\quad(38)$$

To gain a better understanding of the role of multiplicative noise, it would be useful to explore in further detail the mechanical analogy of our basic equation (5). We now regard the critical current J_c as being a telegraph signal (dichotomous noise), which jumps at random times between the two fixed values, J_{c1} and J_{c2}. In terms of an overdamped driven pendulum, a particle moves in the washboard potentials $V_1=-J\varphi-J_{c1}\cos(\varphi)$ and $V_2=-J\varphi-J_{c2}\cos(\varphi)$. The dynamics of the particle motion are fully defined by the value of the driving force J. For $J>J_{c1},J_{c2}$, the motion along both potentials is a continuous descent, and the mobility $\langle\dot\varphi\rangle$ is defined by both potentials. In the limiting case of very large J, according to Eq. (4), one gets $\langle\dot\varphi\rangle=J$. If $J_{c1}<J<J_{c2}$, the motion downhill will be slower since the continuous descent in the potential field V_1 will be interrupted by jumps to the second washboard potential V_2, where, for some time, the motion will be represented by small oscillations near one of the minima of V_2, before returning to V_1. Finally, for $J<J_{c1},J_{c2}$, both motions comprise small oscillations around local minima, which means that $\langle\dot\varphi\rangle=0$.

The typical graphs of the voltage-current characteristics for multiplicative dichotomous noise are shown in Figs. 1, 5, and 6. The last two graphs show the voltage-current characterictic for different noise rates and amplitudes of the multiplicative dichotomous noise, respectively. The nonmonotonic behavior of the mobility $\langle\dot\varphi\rangle$ as a function of noise rate β is shown in Fig. 7. Just as for additive noise, this stochastic resonance occurs in narrow region of the bias current J.

A few characteristic features of these graphs obtained for multiplicative noise should be mentioned, which are distinguished from those shown in Figs. 1–4 for additive noise.

(1) No ''ratchet effects'' exist for multiplicative noise even when the latter is asymmetric. (One can show [20] that

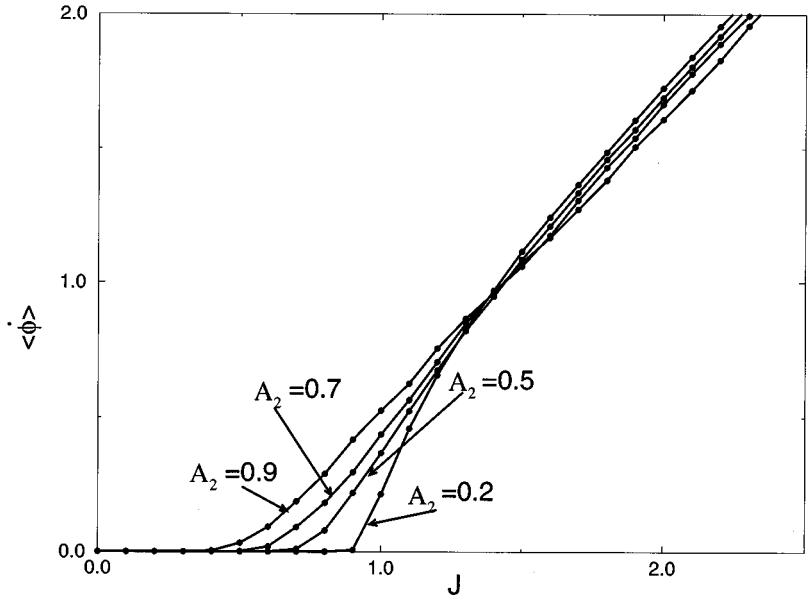

FIG. 5. Voltage-current characteristic of a Josephson junction subject to multiplicative dichotomous noise for different noise amplitudes A_2. Parameters are $J_c=1$ and $\beta=1$.

the rachet effects occur for multiplicative noise when—in our notation—$J_{c1}>0$ but $J_{c2}<0$). The vanishing of $\langle\dot{\varphi}\rangle$ for $J=0$ can be seen not only from Fig. 5 but also from the first equation of (32), which for $J=0$ can be rewritten as $W=(Y-J_c)\sin(\varphi)$. The flux W has to be constant in a stationary state, which means $W=0$ and $\langle\dot{\varphi}\rangle=0$.

(2) In contrast to rachets, the stochastic resonance phenomenon exists for multiplicative dichotomous noise, just as for additive dichotomous noise (Fig. 7).

(3) While the asymptotic form of the current-voltage characteristic of a Josephson junction subject to additive noise obeys Ohm's law, for multiplicative noise the asymptotic differs from Ohm's law, as one can see from Fig. 1. The same results follow from our equations, namely, for $J\gg J_{c1},J_{c2}$, $W=J\langle P\rangle+\langle Y\sin(\varphi)\rangle$, and $\langle\dot{\varphi}\rangle=J+2\pi\langle Y\sin(\varphi)\rangle$, where $Y(\varphi)$ is to be found from Eqs. (32).

V. JOINT ACTION OF MULTIPLICATIVE AND ADDITIVE NOISE

For the general case of both multiplicative and additive noises, one has to solve Eq. (18). The analytic treatment of the general case is too cumbersome. Let us instead discuss the results for some simple cases.

White additive noise and very fast multiplicative dichotomous noise

When the transition rate β of the multiplicative symmetric ($A=|B|$) dichotomous noise is very large, $\beta\to\infty$, the system is subject to the average noise. This means that there is no multiplicative noise at all, i.e., the equation of motion (5) has the following form:

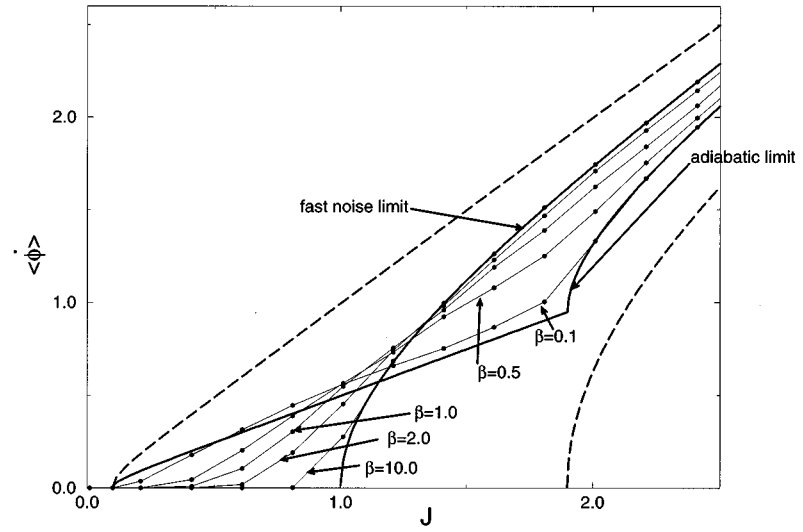

FIG. 6. Same as Fig. 5 but for different values of noise rates β. Parameters are $J_c=1$ and $A_2=B_2=0.9$.

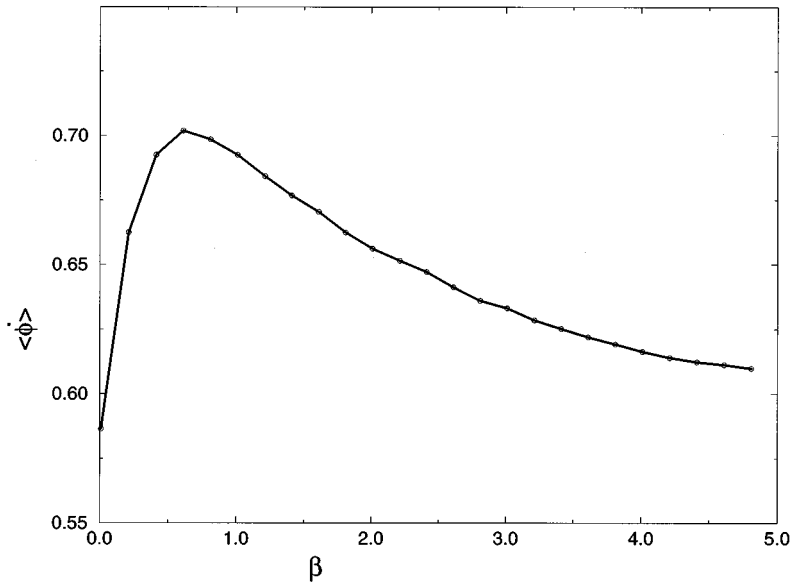

FIG. 7. Voltage $\langle\dot{\varphi}\rangle$ as a function of noise rate β for multiplicative dichotomous noise. Parameters are $A_2=B_2=0.9$ and $J_c=1$.

$$\frac{d\varphi}{dt}=J-J_c\ \sin\ \varphi+f_1(t), \tag{39}$$

where $f_1(t)$ is the white noise. The mobility $\langle\dot{\varphi}\rangle$ for Eq. (39) can be calculated exactly, yielding [23]

$$\langle\dot{\varphi}\rangle=\frac{\sinh(\pi J/D)}{\pi/D}\left|I_{iJ/D}\ \frac{J_c}{D}\right|^{-2}, \tag{40}$$

where $I_{iJ/D}$ is the modified Bessel function of the first order, with imaginary argument and imaginary index [24]. In the limiting case when $J,D\ll 1$, Eq. (40) reduces to [see Eq. (9.56) in Ref. [24]]

$$\langle\dot{\varphi}\rangle=2\ \sinh\ \frac{\pi J}{D}\exp\left(-\frac{2J_c}{D}\right). \tag{41}$$

Each of the two factors in Eq. (41) has a clear physical meaning [25]. The Arrhenius exponential rate, $\exp(-2J_c/D)$, decreases with D, which makes it easier for a system to overcome a potential barrier, while the preexponential factor—the difference between approach to the left well and to the right well—makes the system more homogeneous.

White additive noise and very slow multiplicative dichotomous noise

For very slow processes, $\beta\to 0$, the total voltage is given by the average of the two potentials [21]:

$$\langle\dot{\varphi}\rangle=\frac{1}{(\beta_1+\beta_2)}[\beta_2\langle\varphi\rangle_{J,J_{c_1},D}+\beta_1\langle\varphi\rangle_{J,J_{c_2},D}]. \tag{42}$$

As shown in Ref. [21], Eqs. (40)–(42) define the nonmonotonic behavior of the current $W=2\pi\langle\dot{\varphi}\rangle$ as a function of β, manifesting itself by appearing in both the minimum and the maximum on the graphs.

White additive noise and multiplicative noise

When both noises are white, the following limits apply in the general equations (20)–(23): $A_1,A_2,\alpha,\beta\to\infty$ with $\lim A_1^2/2\alpha=D_1$ and $\lim A_2^2/2\beta=D_2$, which immediately yields Eq. (24) for the probability density function $P(\varphi)$ and, finally, one obtains Eq. (28) for the voltage $\langle\dot{\varphi}\rangle$.

Figure 8 displays $\langle\dot{\varphi}\rangle$ as a function of J when both noises are white. It is remarkable that for weak additive noise ($D_1=0.02$) and strong multiplicative noise ($D_2=10$), the voltage-current characteristic for small J climbs higher than that predicted by Ohm's law.

Multiplicative dichotomous noise and additive white noise

Analogous to the previous case, after excluding the functions X and Z from Eqs. (20)–(23), one obtains the following equations for $P(\varphi)$ and $Y(\varphi)$:

$$\beta Y+\frac{d}{d\varphi}(gY)-D_1\frac{d^2Y}{d\varphi^2}+A_2^2\frac{d}{d\varphi}(P\ \sin\ \varphi)=0, \tag{43}$$

$$W=gP-D_1\frac{dP}{d\varphi}+Y\ \sin\ \varphi. \tag{44}$$

After excluding Y from these two equations, one gets a third-order differential equation for $P(\varphi)$, which cannot be solved analytically. The appropriate equations have been analyzed numerically in Ref. [21].

White multiplicative noise and dichotomous additive noise

Taking the limits $A_2,\beta\to\infty$ such that $\lim A_2^2/2\beta=D_2$, one obtains from Eqs. (22) and (23)

$$Y=-D_2\frac{d}{d\varphi}(P\ \sin\ \varphi),\quad Z=-D_2\frac{d}{d\varphi}(X\ \sin\ \varphi). \tag{45}$$

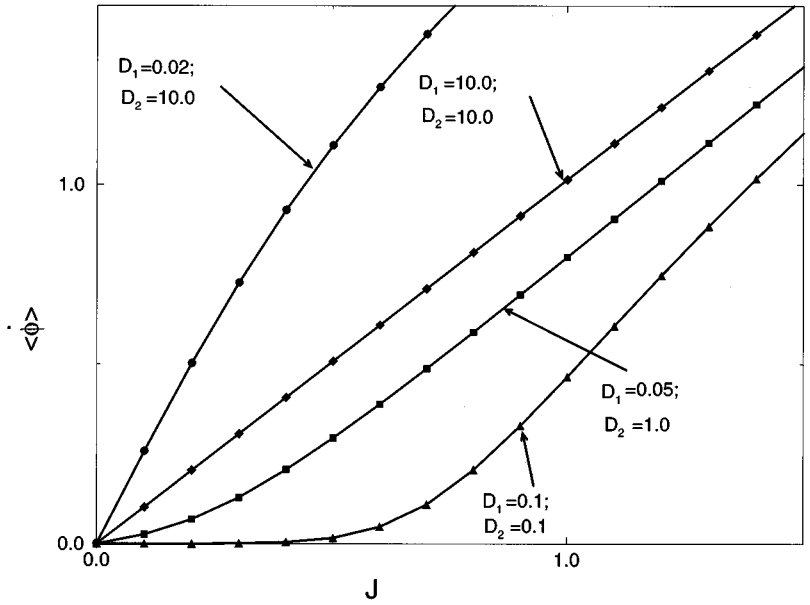

FIG. 8. Voltage-current characteristic of Josephson junction subject to both additive and multiplicative white noises of strengths D_1 and D_2, respectively ($J_c=1$).

Substitution of the latter formula into Eqs. (20) and (21) gives

$$\alpha X+(gX)-A_1^2\frac{dP}{d\varphi}+D_2\frac{d}{d\varphi}\left[\sin\varphi\frac{d}{d\varphi}(X\sin\varphi)\right]=0, \tag{46}$$

$$W=gP+X-D_2\sin\varphi\frac{d}{d\varphi}(P\sin\varphi). \tag{47}$$

Again, the third-order differential equation for $P(\varphi)$, which is obtained from these two equations, allows only a numerical solution. This can be obtained in complete analogy with those performed in Ref. [21].

Multiplicative dichotomous noise and additive dichotomous noise

In this general case one has to solve the four equations of Eq. (18), which can be done only numerically. Results of numerical simulations are shown in Fig. 9 for simultaneous action of symmetric additive and multiplicative dichotomous noises. A few interesting comments are necessary:

(a) None of the noises has any influence on the current-voltage characteristic for $J+A_1<J_c$ (additive noise) and for

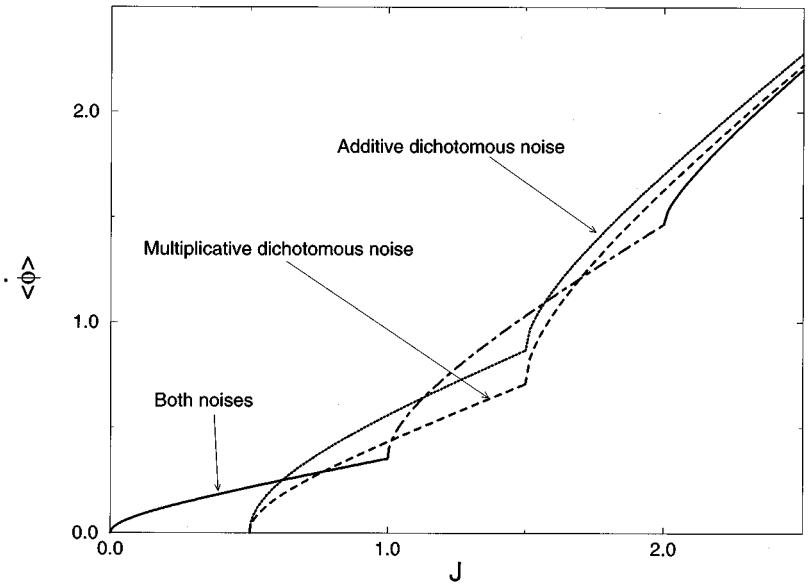

FIG. 9. Voltage-current characteristic of a Josephson junction subject to additive dichotomous (dotted line), multiplicative dichotomous (dashed line), and both noises (solid line). The parameters have the following values : $A_1=B_1=A_2=B_2=0.5$; $\alpha=\beta\to 0$ (adiabatic case).

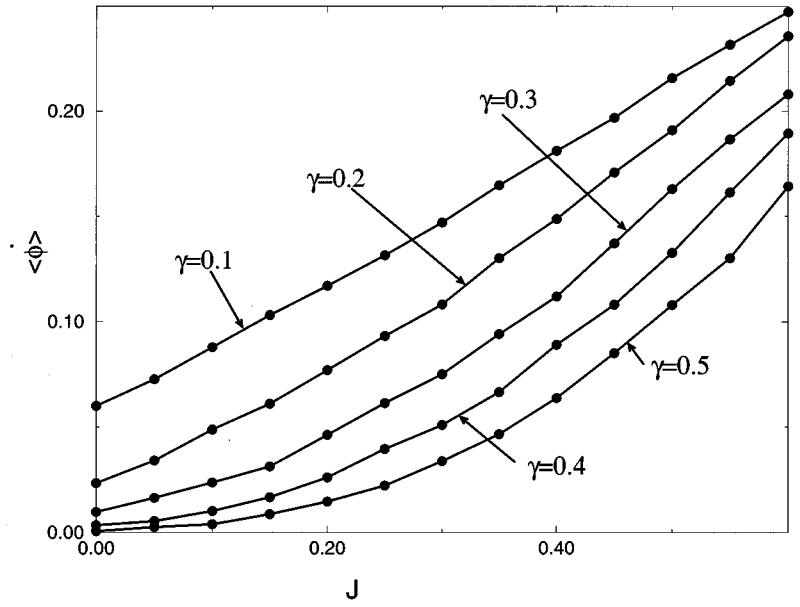

FIG. 10. Voltage-current characteristic of a Josephson junction subject to nonsymmetric additive and symmetric multiplicative dichotomous noises as a function of noise rate γ. The rate γ defines the transition $A_2 \rightarrow -B_2$ and *vice versa* as well as the transition $-B_1 \rightarrow A_1$, while the rate of transition from A_1 to $-B_1$ is equal to 2γ. The parameters have the following values: $A_1=0.9$; $B_1=0.45$; $A_2=B_2=0.5$ and $J_c=1$.

$J<J_c-B_1$ (multiplicative noise), while the common action of both noises changes the current-voltage characteristic even in these regions.

(b) The ''ratchet effect'' (appearance of net voltage $\langle \dot{\varphi} \rangle$ in the absence of driving current, $J=0$) exists for nonsymmetric additive dichotomous noise even in the presence of symmetric multiplicative dichotomous noise, as one can see from Figs. 10 and 11. Moreover, multiplicative noise eases the criteria for the onset of the ratchet effect. The conditions $J>A_1$ and $J>B_1$ that appear in the absence of multiplicative noise are no longer necessary when multiplicative noise is present.

VI. LIMIT CASES OF WEAK AND STRONG NOISE

In this section we develop a convenient means of analysis for some limiting cases of the formulas, we derived.

The generic equation (24), which we use for the analysis of different types of noise, is a first-order differential equation with periodic coefficients of the following form:

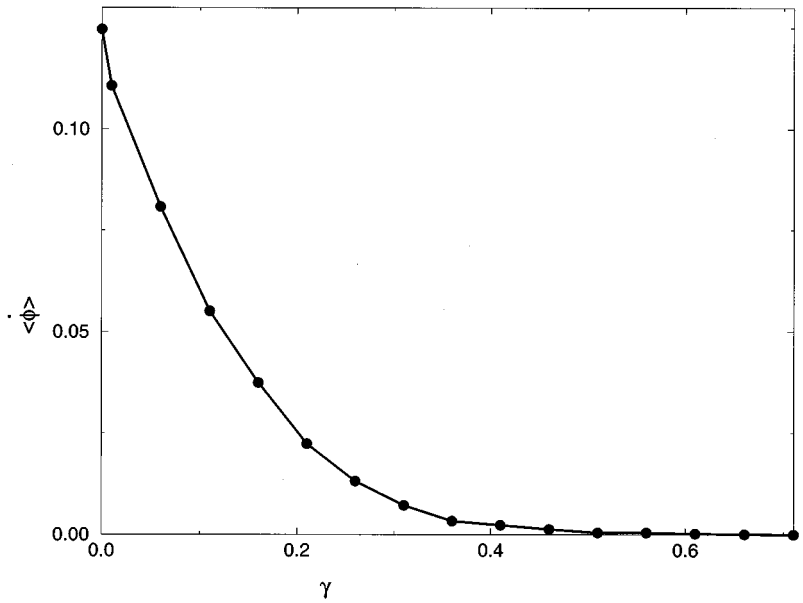

FIG. 11. Voltage $\langle \dot{\varphi} \rangle$ in the absence of the driving force, $J=0$ (''ratchet effect'') as a function of noise rate γ. Parameters are the same as in Fig. 10.

$$P=\Psi(\varphi)P'+W\Phi(\varphi)=\Psi(\varphi)P'+Q(\varphi), \tag{48}$$

where here and in the discussion that follows, the prime denotes the derivative with respect to φ. In some cases the functions $\Psi(\varphi)$ and $\Phi(\varphi)$ have singularities, or the function $\Psi(\varphi)$ vanishes at some φ. In the latter case, one has to use singular perturbation theory. However, the function $P(\varphi)$ must be periodic and normalized function of φ. We use this fact to simplify some series expansions and approximations.

Let us integrate Eq. (48) over a period and continue integration by parts on the right side of this equation:

$$1=\oint Q+\oint \Psi P'=\oint Q-\oint Q\Psi'-\oint \Psi'\Psi P'=\cdots . \tag{49}$$

If we define the operator $O_\Psi(\varphi)\equiv(\Psi\varphi)'$, we obtain

$$1=\oint Q[1-O_\Psi(1)+O_\Psi(O_\Psi(1))-\cdots].$$

Taking into account that $W\Phi(\varphi)=Q(\varphi)$, one can rewrite this operator series in a more compact form

$$W=\left\{\oint \Phi\left(\left[\frac{1}{1-O_\Psi}\right](1)\right)\right\}^{-1} \tag{50}$$

or

$$W=\frac{1}{\oint \Phi(1-\Psi'+(\Psi\Psi')'-[\Psi(\Psi\Psi')]'+\cdots)}. \tag{51}$$

This form of solution of Eq. (48) is very convenient when the function $\Psi(\varphi)$ in Eq. (48) vanishes at some φ and one has to use singular perturbation theory. However, such an expansion is not convenient when the coefficient in front of P is equal to zero. Then, the functions Φ and Ψ have singularities and Eq. (50) is of no use. For these cases we use another representation of the solution for Eq. (48) by rewriting Eq. (48) in the following form:

$$P'-\frac{\Theta(\varphi)}{D}P=W\Omega(\varphi). \tag{52}$$

Using periodicity and normalization of P yields the following form of solution for the current W:

$$W=\left[\int_0^{2\pi}\frac{e^{(1/D)\int_0^\varphi\Theta(z)dz}}{e^{-(1/D)\int_\varphi^{\varphi+2\pi}\Theta(z)dz}-1}\left(\int_\varphi^{\varphi+2\pi}\Omega(\xi)e^{-(1/D)\int_0^\xi\Theta(z)dz}d\xi\right)d\varphi\right]^{-1}. \tag{53}$$

If Θ is a periodic function plus constant, the value of $\int_\varphi^{\varphi+2\pi}\Theta(z)dz$ will not depend on φ, and the last integral reduces to some constant k. Then Eq. (53) is simplified,

$$W=(e^{-k/D}-1)\left[\int_0^{2\pi}e^{(1/D)\int_0^\varphi\Theta(z)dz}\left(\int_\varphi^{\varphi+2\pi}\Omega(\xi)e^{-(1/D)\int_0^\xi\Theta(z)dz}d\xi\right)d\varphi\right]^{-1}. \tag{54}$$

In the limit of $D\to 0$, one can use the method of steepest descent for calculating the integrals in Eqs. (53) and (54), which gives

$$W=\frac{(e^{-k/D}-1)\sqrt{|\Theta'(x_1)\Theta'(x_2)|}}{2\pi D\Omega(x_2)}e^{(1/D)\int_{x_1}^{x_2}\Theta(z)dz}, \tag{55}$$

where x_1 and x_2 are two neighboring zeros of $\Theta(x)$, where $x_2>x_1$, and $\Theta'(x_1)<0$, $\Theta'(x_2)>0$. Note that Eq. (55) cannot be expanded in series, in contrast to Eq. (50). Finally, since $(e^{-k/D}-1)\approx -1$ for $D\to 0$, one obtains

$$W=-\frac{\sqrt{|\Theta'(x_1)\Theta'(x_2)|}}{2\pi D\Omega(x_2)}e^{(1/D)\int_{x_1}^{x_2}\Theta(z)dz}. \tag{56}$$

If $\Theta(z)$ is of order zero in D, one can also consider the opposite limiting case of $D\to\infty$, rewriting Eq. (54) in the form

$$W=\sum_{t=1}^{\infty}\left[-\frac{k}{D}\right]^t\left[\sum_{n,m=0}^{\infty}\int_0^{2\pi}\left[\frac{1}{D}\int_0^\varphi\Theta(z)dz\right]^m\left(\int_\varphi^{\varphi+2\pi}\Omega(\xi)\left[-\frac{1}{D}\int_0^\xi\Theta(z)dz\right]^n d\xi\right)d\varphi\right]^{-1}. \tag{57}$$

Equation (57) gives the expansion of the current W for large D. If Θ is a periodic function plus some constant, the first term of this expansion is

$$W \sim -\frac{\int_0^{2\pi}\Theta(z)dz}{2\pi D\int_0^{2\pi}\Omega(z)dz}. \tag{58}$$

Applications of the derived formulas will be illustrated by the examples of one and two white noises.

White additive noise

The general formula (28) can be simplified for weak and strong noise strengths. For $D\to\infty$, one obtains

$$\langle\dot{\varphi}\rangle \sim J\left(1-\frac{J_c^2}{2D^2}+\frac{J_c^2(16J^2+5J_c^2)}{32D^4}+\cdots\right). \tag{59}$$

Notice that the correction terms are proportional to $(J_c/D)^2$, which means that for large additive white noise, the correction terms to Ohm's law, $\langle\dot{\varphi}\rangle\sim J$, are very small.

The voltage-current characteristic is of greatest interest for weak noise. Following the general approach given at the beginning of this section, for $D\to 0$, all calculations have to be separated into two parts. In the case $J>J_c$, we can use Eq. (50) to obtain the first correction to Eq. (4):

$$\langle\dot{\varphi}\rangle \sim \sqrt{J^2-J_c^2}+D^2J_c^2\frac{J_c^2+4J^2}{8(J^2-J_c^2)^{5/2}}+\cdots \quad \text{for} \quad J>J_c. \tag{60}$$

Equation (60) contains corrections to Eq. (4) that are proportional to $(DJ_c)^2$, similar to the corrections of order $(J_c/D)^2$ in Eq. (59). However, the situation is quite different for $J<J_c$. We now have to use Eqs. (55) and (56), rather than Eq. (50). In terms of the characteristic frequencies

$$\omega_1=\sqrt{J_c^2-J^2}, \quad \omega_2=2[\omega_1-J\ \arccos(J/J_c)] \tag{61}$$

the weak noise correction is

$$\langle\dot{\varphi}\rangle \sim \omega_1 e^{-\omega_2/D} \quad \text{for} \quad J<J_c. \tag{62}$$

Note that Eq. (62) has been obtained under the condition of small D, so that J and J_c are larger than D. For $J<D$, Eq. (62) gives an incorrect result whereas the correct result is $\langle\dot{\varphi}\rangle\simeq 0$.

We conclude, therefore, that in two regions, $J<J_c$ and $J>J_c$, the corrections for small D have different forms, changing from an exponential form (62) to a polynomial form (60). Such behavior of the solution of the nonlinear equation (1) is a manifestation of the change from flow-type motion to Arrhenius-type jumps.

White additive noise and multiplicative noise

Analogous to the calculations performed above, one can find the limiting forms of Eqs. (27) for small and large noise strengths D_1 and D_2. For small D, the corrections have different forms in the two regions $J<J_c$ and $J>J_c$. For $J>J_c$ (''the flow region'')

$$\langle\dot{\varphi}\rangle \sim \sqrt{J^2-J_c^2}+D^2\frac{J_c^4+4J^2J_c^2+R^2J^4+10RJ^2J_c^2+4R^2J^2J_c^2}{8(J^2-J_c^2)^{5/2}}, \tag{63}$$

where $D_2=RD_1$, and R is assumed to be of order unity.

For the Arrhenius region, $J<J_c$, the small D corrections to the voltage-current characteristic have the following form:

$$\langle\dot{\varphi}\rangle \sim \omega_1 e^{-(2J/D\sqrt{1+R})\arctan(J\sqrt{1+R}/\omega_1)}\left[\frac{1+\xi}{1-\xi}\right]^{-b/D\sqrt{R(1+R)}}, \tag{64}$$

where ω_1 and ξ are defined by

$$\omega_1=\sqrt{J_c^2-J^2},$$
$$\xi=\sqrt{\frac{R}{R+1}}\frac{\omega_1}{J_c}. \tag{65}$$

Several differences between Eqs. (63) and (64) and the appropriate equations (60) and (62) in the absence of the multiplicative noise are worthy of notice.

Firstly, the boundary between the flow region and the Arrhenius region, which in the former case was simply defined by $J=J_c$, becomes more complicated and, in fact, the boundary between the applicability of Eqs. (63) and (64) is defined by $J-J_c\sin(\varphi)-(DR/2)\sin(2\varphi)=0$. The second difference between Eqs. (60) and (63) is that in the latter equation the correction terms do not vanish for $J_c\to 0$, which may have much to do with the presence of multiplicative noise. One can also find the limiting form of Eq. (27) for large noise strength, $D\to\infty$:

$$\langle\dot{\varphi}\rangle \sim \frac{\pi^2 J}{4\sqrt{1+R}[\int_0^{\pi}dx/\sqrt{1+R\ \sin^2(x)}]^2}. \tag{66}$$

One can see from this equation that the current-voltage characteristic is changing drastically due to the presence of multiplicative white noise. Instead of small corrections to Ohm's law due to additive white noise, Eq. (59), multiplicative noise leads to significant changes even in leading order. This change can be essential for large values of R. For example, for $R=500$, the influence of multiplicative noise leads to $\langle\dot{\varphi}\rangle\sim 2.37J$, which explain the strong slope in Fig. 8 for $D_1=0.02$ and $D_2=10$. For smaller values of R, the slope is approaching that of Ohm's law, and finally, for $R=0$, we come back to Ohm's law.

VII. CONCLUSIONS

Our main results concern the voltage-current characteristics of a Josephson junction subject to additive and multiplicative noises, which we have chosen as dichotomous noises, although in the Appendix we present the Fokker-Planck equations for the more general case of exponentially correlated noises. Results of our investigation can be summarized in the following way:

Multiplicative noise alone (random distribution of critical currents or some other external noises)

(a) We obtained an analytic solution for the voltage-current characteristic [Eq. (40)].

(b) Asymptotic behavior of the voltage-current characteristic for $J\to\infty$ is different from Ohm's law (Fig. 1).

(c) The voltage increases with noise amplitude for small currents. However, for larger currents, the voltage decreases with noise amplitude (Fig. 5).

(d) Near this transient region, the voltage turns out to be a nonmonotonic function of the noise rate (Fig. 7), which is one of the manifestations of stochastic resonance.

(e) In contrast to additive noise, even nonsymmetric multiplicative noise is unable to produce the ''ratchet effect'' (net voltage in the absence of biased current).

Additive noise alone (thermal or some other internal noise)

This case was analyzed previously [1,6–8]. We considered a relationship between the form of the current-voltage characteristic and noise rate and amplitude, and found the following.

(a) The voltage-current characteristics for different noise rates are confined between the two limits of fast and slow noises (Fig. 2) and occupy a small amount of space between the voltage-current characteristics of two separate states. The latter (adiabatic) case can be calculated analytically [Eq. (31)].

(b) The stochastic resonance (the nonmonotonic behavior of voltage as a function of noise rate) occurs in a wider range of currents than that for multiplicative noise (Figs. 2 and 3).

(c) Just as for multiplicative noise, the voltage increases with noise amplitude for small current and decreases for large current (Fig. 3).

Simultaneous action of additive and multiplicative noises

(a) Two dichotomous noises are able to produce voltages for small currents (Fig. 9) while each by itself is unable to give non-zero voltage in this region of current.

(b) The cooperative effect mentioned above occurs also for two white noises. Moreover, the resulting voltage can be larger than that in Ohm's law if the additive noise is weak and the multiplicative noise is strong (Fig. 8).

(c) The simultaneous action of two noises can be larger than each by itself in some region of the voltage-current characteristic, but smaller in other regions.

(d) The ''ratchet effect'' occurs for nonsymmetric additive noise in the presence of multiplicative noise (Figs. 10 and 11). The latter eases the requirments for the onset of ratchets.

Analysis of limiting cases of weak and strong noises

(a) We suggested a convenient method of analysis of these limiting cases when the Fokker-Planck equations contain singularities.

(b) The small-D corrections to the voltage generated by additive noise have a polynomial form in the flow-type region, $J>J_c$, and an exponential form in the Arrhenius-type region, $J<J_c$.

(c) The same effect occurs when both additive and multiplicative white noises are present, with the boundary between the flow-type and Arrhenius-type regions shifted to $J<J_c$.

APPENDIX

Here we present a slightly more general set of stochastic equations corresponding to the Langevin equation (5) for any two independent exponentially correlated zero-mean noises:

$$\langle f_i(t)f_i(t')\rangle=\sigma_i^2\ \exp[-\lambda_i|t-t'|], \tag{A1}$$

$$\langle f_i(t)\rangle=0, \tag{A2}$$

$$\langle f_1(t)f_2(t')\rangle=0. \tag{A3}$$

The probability density function $P(\varphi,t)$ is defined as the statistical average of the Dirac function $\rho(\varphi,t)=\delta(\varphi-\varphi(t))$, namely, $P(\varphi,t)=\langle\rho(\varphi,t)\rangle$ [19]. Then, the stochastic Liouville equation has the following form:

$$\frac{\partial\rho}{\partial t}=-\frac{\partial}{\partial\varphi}\{[g(\varphi)+f_1-f_2\ \sin(\varphi)]\rho\}, \tag{A4}$$

where $g(\varphi)$ was defined in Eq. (16), and the appropriate Fokker-Planck equation is

$$\dot P=-\frac{\partial}{\partial\varphi}[g(\varphi)P+\langle\rho f_1\rangle-\langle\rho f_2\rangle\sin(\varphi)]. \tag{A5}$$

Multiplying Eq. (A4) by f_1, f_2 and f_1f_2, respectively, and averaging the resulting equations, one obtains the Fokker-Planck equations for the functions,

$$X=\langle\rho f_1\rangle,\quad Y=\langle\rho f_2\rangle,\quad Z=\langle\rho f_1f_2\rangle. \tag{A6}$$

The time derivatives of these functions, which appear on the left-hand side of the Fokker-Planck equations, can be simplified for the random functions (A1) by use of the well-known Shapiro-Logunov formula [16]:

$$\frac{\partial}{\partial t}\langle\alpha(t)\varphi[\alpha]\rangle=\left\langle\alpha(t)\frac{d}{dt}\varphi[\alpha]\right\rangle-\lambda\langle\alpha(t)\varphi[\alpha]\rangle, \tag{A7}$$

where $\varphi[\alpha]$ is a functional of the random value $\alpha(t)$, and the average is performed over the distribution of $\alpha(t)$.

Finally, we come to the following set of equations:

$$\begin{aligned}
\dot P&=-[Pg(\varphi)+X-Y\ \sin(\varphi)]',\\
\dot X&=-\lambda_1X-[g(\varphi)X+\langle\rho f_1^2\rangle-Z\ \sin(\varphi)]',\\
\dot Y&=-\lambda_2Y-[g(\varphi)Y-\langle\rho f_2^2\rangle\sin(\varphi)+Z]',\\
\dot Z&=-(\lambda_1+\lambda_2)Z-[g(\varphi)Z+\langle\rho f_1^2f_2\rangle-\langle\rho f_1f_2^2\rangle\sin(\varphi)]'.
\end{aligned} \tag{A8}$$

The system of equations (A8) contains the averages $\langle\rho f_1^2f_{2\rangle}$ and $\langle\rho f_1f_2^2\rangle$ and, therefore, this system is not closed. One has to use some decoupling procedure. Another possibility that we demonsrate in this work is to consider the special case of the two-state Markov process. For symmetric

dichotomous noise $f_1^2(t)=A_1^2$ and $f_2^2(t)=A_2^2$ and Eq. (A8) reduces to Eqs. (20)–(23). For nonsymmetric dichotomous noise one can easily obtain

$$\langle \rho f_1^2 \rangle = A_1 B_1 P + (A_1 - B_1) X,$$

$$\langle \rho f_2^2 \rangle = A_2 B_2 P + (A_2 - B_2) Y,$$

$$\langle \rho f_1^2 f_2 \rangle = A_1 B_1 Y + (A_1 - B_1) Z,$$

$$\langle \rho f_2^2 f_1 \rangle = A_2 B_2 X + (A_2 - B_2) Z. \tag{A9}$$

Substitution of Eq. (A9) into Eq. (A8) gives Eq. (18).

[1] A. Barone and G. Paterno, *Physics and Applications of the Josephson Effect* (John Wiley, New York, 1982).

[2] G. Grüner, A. Zawadowski, and P. M. Chaikin, Phys. Rev. Lett. **46**, 511 (1981).

[3] A. J. Viterbi, *Principles of Coherent Communications* (McGraw-Hill, New York, 1966).

[4] W. Schleich, C. S. Cha, and J. D. Cresser, Phys. Rev. A **29**, 230 (1984).

[5] B. Shapiro, I. Dayan, M. Gitterman, and G. H. Weiss, Phys. Rev. B **46**, 8416 (1992).

[6] B. Chen and J. Dong, Phys. Rev. B **44**, 10 206 (1991).

[7] G. Weiss and M. Gitterman, J. Stat. Phys. **70**, 93 (1993).

[8] M. M. Millonas and D. R. Chialvo, Phys. Rev. E **53**, 2239 (1996).

[9] G. Blatter, M. V. Feigelman, V. B. Geshkenbein, A. I. Larkin, and V. M. Vinokur, Rev. Mod. Phys. **66**, 1125 (1994).

[10] M. J. Ferrary, J. J. Kingston, F. C. Wellstood, and J. Clarke, Appl. Phys. Lett. **58**, 1106 (1991); M. J. Ferrary *et al.*, Phys. Rev. Lett. **64**, 72 (1990).

[11] G. Jung, B. Say, L. Maritato, S. Prishepa, C. Attanesio, and A. Vecchiane, in *Progress in High-T_c Superconductivity*, edited by Baran, W. Gorzowsky, and H. Szymczak (World Scientific, Singapore, 1992), Vol. 30, p. 192.

[12] G. Jung, S. Vitale, J. Konorka, and M. Bonaldi, J. Appl. Phys. **70**, 5440 (1991).

[13] G. Jung, B. Savo, A. Veccione, and G. Attanasio, Cryogenics **32**, 1093 (1992).

[14] M. Johnson, M. J. Ferrary, F. C. Wellstood, J. Clarke, M. R. Beasley, A Inam, X. D. Wu, L. Nazar, and T. Venkatesan, Phys. Rev. B **42**, 10 792 (1990).

[15] G. Jung, B. Savo, and A. Vecciano, Europhys. Lett. **21**, 947 (1993).

[16] V. E. Shapiro and V. M. Loginov, Physica A **91**, 563 (1978).

[17] Van den Broeck, J. Stat. Phys. **31**, 467 (1983).

[18] J. Łuczka, R. Bartussek, and P. Hänggi, Europhys. Lett. **31**, 431 (1995).

[19] N. G. Van Kampen, Phys. Rep. **24**, 171 (1976).

[20] V. Berdichevsky and M. Gitterman, Physica A (to be published).

[21] S. Park, S. Kim, and C. Ryu, Phys. Lett. A **225**, 245 (1997).

[22] C. R. Doering and J. C. Gadoua, Phys. Rev. Lett. **69**, 2318 (1992).

[23] R. L. Stratonovich, *Topics in the Theory of Random Noise*, Vol. II (Gordon and Breach, New York, 1967), p. 241.

[24] L. S. Gradstein and I. M. Ryzhik, *Tables of Integrals, Series and Products* (Academic, New York, 1994).

[25] M. Gitterman, I. B. Khalfin, and B. Ya. Shapiro, Phys. Lett. A **184**, 339 (1994).